

## INDIRECT FIELD ORIENTATION CONTROL OF INDUCTION MACHINE WITH DETUNING EFFECT

Khalaf S. K. Al-Shemari

Assistant Lecturer

Electrical Eng. Dept.-University of Tikrit

### ABSTRACT

Induction motors (IM) are characterized by complex, highly nonlinear, time varying dynamics and inaccessibility of some states and outputs for measurements and hence may be considered as a challenging problem.

Field orientation control (FOC) methods of an induction machine achieve decoupled torque and flux dynamics leading to independent control of torque and flux as for separately excited DC motor, but they are sensitive to motor parameter variations. The present work select the indirect field orientation control (IFOC) as an effective method for eliminating the coupling effect. The results showed how well the drive performance has been improved by this control strategy. However, to what extent the control strategy can perform the decoupling relies on the accuracy of the slip frequency calculation. Unfortunately, the slip frequency depends on the rotor time constant that varies continuously according to the operational conditions and, then, the coupling effect may again arise.

This paper investigates the improvement in the performance of the induction machine dynamics as the IFOC technique is utilized. Also, it investigates the degradation in dynamic performance when the rotor resistance is deviated from its nominal value.

## INTRODUCTION

The fundamentals of vector control implementation can be explained with the help of Fig.(1), where the machine model is presented in a synchronous rotating reference frame. The inverter is omitted from the figure, assuming that it has unity current gain, that is, it generates currents  $i_a$ ,  $i_b$ , and  $i_c$  as dictated by the corresponding command currents  $i_a^*$ ,  $i_b^*$ , and  $i_c^*$  from the controller. A machine model with internal conversions is shown on the right. The machine terminal phase currents  $i_a$ ,  $i_b$ , and  $i_c$  are converted to  $i_{ds}^s$  and  $i_{qs}^s$  components by  $3\phi/2\phi$  transformation. These are then converted to synchronously rotating frame by the unit vector components  $\cos\theta_e$  and  $\sin\theta_e$  before applying them to the  $d^e - q^e$  machine model. The controller makes two stages of inverse transformation, as shown, so that the control currents  $i_{ds}^{e*}$  and  $i_{qs}^{e*}$  correspond to the machine currents  $i_{ds}^e$  and  $i_{qs}^e$ , respectively. In addition, the unit vector assures correct alignment of  $i_{ds}^e$  with the  $\lambda_r'$  and  $i_{qs}^e$  perpendicular to it, as shown in Fig.(1). The transformation and inverse transformation including the inverter ideally do not incorporate any dynamics and therefore, the response to  $i_{ds}^e$  and  $i_{qs}^e$  is instantaneous (neglecting computational and sampling delays).

There are two essentially general methods of vector control; one called the direct method, and the other known as the indirect method. The methods are different essentially by how the unit vector ( $\cos\theta_e$  and  $\sin\theta_e$ ) is generated for the control. It should be mentioned that the orientation of  $i_{ds}^e$  with the rotor flux  $\lambda_r'$ , air gap flux, or stator flux is possible in vector control. However,

rotor flux orientation gives natural decoupling control, whereas air gap or stator flux orientation gives a coupling effect which has to be compensated by a decoupling compensation current [1,2].

### INDIRECT FIELD ORIENTATION CONTROL (IFOC)

Indirect vector control is very popular in industrial applications. Figure (2) explains the fundamental principle of indirect vector control with the help of a phasor diagram. The  $d^s - q^s$  axes are fixed on the stator, but the  $d^r - q^r$  axes, which are fixed on the rotor, are moving at speed  $\omega_r$ . Synchronously rotating axes  $d^e - q^e$  are rotating ahead of the  $d^r - q^r$  axes by the positive slip angle  $\theta_{sl}$  corresponding to slip frequency  $\omega_{sl}$ . Since the rotor pole is directed on the  $d^e$  axis and  $\omega_e = \omega_r + \omega_{sl}$ , one can write

$$\theta_e = \int \omega_e dt = \int (\omega_r + \omega_{sl}) dt = \theta_r + \theta_{sl} \dots\dots\dots(1)$$

The phasor diagram suggests that for decoupling control, the stator flux component of current  $i_{ds}^e$  should be aligned on the  $d^e$  axis, and the torque component of current  $i_{qs}^e$  should be on the  $q^e$  axis, as shown in Fig (2).

For decoupling control, one can make a derivation of control equations of indirect vector control with the help of  $d^e - q^e$  dynamic model of induction machine (IM) [1,2,3,4],

$$\left. \begin{aligned} v_{qr}^{e} &= p\lambda_{qr}^{e} + (\omega_e - \omega_r)\lambda_{dr}^{e} + r_r' i_{qr}^{e} \\ v_{dr}^{e} &= p\lambda_{dr}^{e} - (\omega_e - \omega_r)\lambda_{qr}^{e} + r_r' i_{dr}^{e} \end{aligned} \right\} \dots\dots\dots(2)$$

$$\left. \begin{aligned} v_{qs}^e &= p\lambda_{qs}^e + \omega_e \lambda_{ds}^e + r_s i_{qs}^e \\ v_{ds}^e &= p\lambda_{ds}^e - \omega_e \lambda_{qs}^e + r_s i_{ds}^e \\ T_{em}^e &= \frac{3P}{2} (\lambda_{qr}^e i_{dr}^e - \lambda_{dr}^e i_{qr}^e) \end{aligned} \right\} \dots\dots\dots(3)$$

If  $d^e$ -axis is aligned with the rotor field, the q-component of the rotor field,  $\lambda_{qr}^e$ , in the chosen reference frame would be zero [1,2,5,6],

$$\lambda_{qr}^e = L_m i_{qs}^e + L_r' i_{qr}^e = 0 \dots\dots\dots(4)$$

$$i_{qr}^e = -\frac{L_m}{L_r'} i_{qs}^e \dots\dots\dots(5)$$

With  $\lambda_{qr}^e$  zero, the equation of the developed torque, Eq.(3), reduces to

$$T_{em} = \frac{3P}{2} \frac{L_m}{L_r} \lambda_{dr}^e i_{qs}^e \dots\dots\dots(6)$$

which shows that if the rotor flux linkage  $\lambda_{dr}^e$  is not disturbed, the torque can be independently controlled by adjusting the stator q component current,  $i_{qs}^e$ .

For  $\lambda_{qr}^e$  to remain unchanged at zero, its time derivative ( $p\lambda_{qr}^e$ ) must be zero, one can show from Eq.(2) [6,1,2]

$$\lambda_{dr}^e = \frac{r_r' L_m}{r_r' + L_r' p} i_{ds}^e \dots\dots\dots(7)$$

$$\omega_{sl}^e = \omega_e - \omega_r = \frac{r_r' i_{qs}^e}{L_r' i_{ds}^e} \dots\dots\dots(8)$$

To implement the indirect vector control strategy, it is necessary to use the condition in Eq.s(6), (7), and (8) in order to satisfy the condition for proper orientation. Torque can be controlled by regulating  $i_{qs}^e$  and slip speed  $\omega_{sl}$ .

Given some desired level of rotor flux,  $\lambda_r^*$ , the desired value of  $i_{ds}^{e*}$  may be obtained from,

$$\lambda_{dr}^{e*} = \frac{r_r' L_m}{r_r' + L_r' p} i_{ds}^{e*} \dots\dots\dots (9)$$

For the desired torque of  $T_{em}^*$  at the given level of rotor flux, the desired value of  $i_{qs}^{e*}$  in accordance with Eq.(6) is

$$T_{em}^{e*} = \frac{3}{2} \frac{P}{2} \frac{L_m}{L_r'} \lambda_{dr}^{e*} i_{qs}^{e*} \dots\dots\dots (10)$$

When the field is properly oriented,  $i_{dr}^{e*}$  is zero,  $\lambda_{dr}^{e*} = L_m i_{ds}^{e*}$ : thus, the slip speed of Eq.(8) can be written as

$$\omega_{sl}^{e*} = \omega_e - \omega_r = \frac{r_r'}{L_r'} \frac{i_{qs}^{e*}}{i_{ds}^{e*}} \dots\dots\dots (11)$$

Thus, the above analysis shows that the vector control strategy can provide the same performance as is achieved from a separately excited DC machine; this is done by formulating the stator current phasor, in the two-axis synchronously rotating reference frame, to have two components: magnetizing current component and torque producing current component. The generated motor torque is the product of two current components. By keeping the magnetizing current component at a constant rated value, the motor torque is linearly proportional to the torque-producing component, which is quite similar to the control of a separately excited DC motor [7,8,9].

Figure (3) shows an indirect field-oriented control scheme for a current controlled PWM induction machine motor drive. The command values for the abc stator currents can then be computed as follows

$$\left. \begin{aligned} i_{qs}^{s*} &= i_{qs}^e \cos \theta_e + i_{ds}^e \sin \theta_e \\ i_{ds}^{s*} &= -i_{qs}^e \sin \theta_e + i_{ds}^e \cos \theta_e \end{aligned} \right\} \dots\dots\dots(12)$$

$$\left. \begin{aligned} i_{as}^* &= i_{qs}^{s*} \\ i_{bs}^* &= -(1/2)i_{qs}^{s*} - (\sqrt{3}/2)i_{ds}^{s*} \\ i_{cs}^* &= -(1/2)i_{qs}^{s*} + (\sqrt{3}/2)i_{ds}^{s*} \end{aligned} \right\} \dots\dots\dots(13)$$

### 3. Indirect Field Orientation Detuning:

The success of FOC is based on the proper division of stator current into two components. Using the above d-q axis orientation approach, these two currents components are  $i_{ds}^*$  and  $i_{qs}^*$ , which specify the magnetizing flux and torque respectively [1,2,4,10].

The indirect FOC method uses a feedforward slip calculation, Fig.(3), to partition the stator current. The slip speed equation is rearranged as:

$$\omega_{sl} = \frac{L_m i_{qs}^{e*}}{T_r \lambda_r'} \dots\dots\dots(14)$$

where  $\lambda_r' = L_m i_{ds}^{e*}$ . The above condition, if satisfied, ensures the decoupling torque and flux production; a change in  $i_{qs}^{e*}$  will not disturb the flux and the instantaneous torque control is achieved. This indicates that an ideal field orientation occurs. To what extent this decoupling is actually achieved will depend on the accuracy of motor parameters used. It is easy to be noted that the calculation of the slip frequency in Eq.(14) depends on the rotor resistance. Owing to saturation and heating, the rotor resistance changes and hence the

slip frequency is either over or under estimated. Eventually, the rotor flux  $\lambda_{dr}^e$  and the stator-axis current  $i_{qs}^e$  will be no longer decoupled in Eq.(10) and the instantaneous torque control is lost. Furthermore, the electromechanical torque generation is reduced at steady state under the plant parameter variations and hence the machine will work in a low-efficiency region. Finally, the variation of the parameters of moment of inertia  $J$  and the friction constant  $B$  is common in real applications. For instance, the bearing friction will change after the motor has run for a period of time <sup>[11]</sup>.

Since the values of rotor resistance and magnetizing inductance are known to vary somewhat more than the other parameters, on-line parameter adaptive techniques are often employed to tune the value of these parameters used in an indirect field-oriented controller to ensure proper operation <sup>[2,11,12]</sup>. The detuning effect, generally, causes degradation in the drive performance.

## **SIMULATED RESULTS**

### **1. Simulation of Fixed Voltage Open-Loop Operation:**

The model equations of the IM, Eq.(2), in the stationary qd reference frame are modeled using SIMULINK <sup>[13,14]</sup>. The simulation is set up for simulating the dynamic behavior of the motor with fixed-step type of step size (2e-6 sec). The results from these open-loop operations will later be used as a benchmark to compare the performance of the same motor operated with field-oriented control.

In the model, three-phase voltages of base frequency ( $f_b=50$  Hz) applied to the input are converted into two-phase stationary reference frame

voltages. Once d-q phase voltages obtained, the associated flux and current are calculated and then applied to electromechanical and mechanical torque equations to obtain torque-speed responses.

Based on the stationary reference frame model, Fig.(4) shows the waveforms of stator a-phase voltage,  $v_{ag}$ , the quadrature stator current,  $i_{qs}$ , the developed torque,  $T_{em}$ , and the rotor speed  $\omega_r$  at no-load for a 20-hp motor. The figure shows that the speed is settled at approximately 0.2 sec., which is the same settling time for the stator current and developed torque. Also, the speed has a steady state value of 188.5 rad/sec., as shown. Torque vs. speed curve obtained from the same model is shown in Fig.(5) for no-load condition.

The value of the externally applied mechanical torque is generated by a repeating sequence source with the time and output values scheduled as follows:

Time array :time\_tmech = [0 0.75 0.75 1.0 1.0 1.25 1.25 1.5 1.5 2].

Output array: tmech\_tmech = [0 0 -Trated -Trated -Trated/2 -Trated/2 -Trated -Trated 0 0].

Sample results showing the starting of the motor with full stator voltage and the response of the motor to the programmed sequence of loading are shown in Fig.(6). In the figure, the speed is expressed in per unit (p.u.) and the speed settled to unity. Also, the figure shows the magnitude of stator and rotor

flux linkages per second ( $|\psi_s| = \sqrt{\psi_{qs}^2 + \psi_{ds}^2}$ ) and  $|\psi_r| = \sqrt{\psi_{dr}'^2 + \psi_{qr}'^2}$ , where  $\psi = \omega_b \lambda$  (volt). One can observe the oscillatory response of the rotor flux linkage before it builds up to its steady state value (172.56 V.). The flux response shows a large change when the load is suddenly changed.



## 2. Simulation of IFOC Developed in Stationary Reference Frame

This simulation is implemented to be familiar with indirect field-oriented control and to observe the variables at every stage of the control.

It is easy to build the SIMULINK model for a current regulated PWM IFOC IM of Fig.(3) [13,14,15]. In this simulation, reference  $dq$  currents are obtained according to the reference load torque and speed waveform. These  $dq$  reference currents are transformed into  $abc$  reference currents to be compared with the actual motor currents and the errors are fed to three hysteresis controllers to obtain reference voltages.

The proportional gain  $k_p$  and integral gain  $k_i$  of the speed controller are tuned to give the best speed response shown in Fig.(7). The value of  $k_p=75$  and  $k_i=7$  have been chosen to meet such transient specification. Also, the allowable commanded torque generated from the speed controller should not exceed  $\pm T_{lim}$  (170 N.m), as dedicated by the developed torque response shown in Fig.(5). The look-up table for field weakening matches the desired value of the rotor d-axis flux,  $\lambda_{dr}^e$ , to that of the mechanical speed of the rotor,  $\omega_r$ . For speed less than the base or rated speed,  $\lambda_{dr}^e$  is set equal to its no-load value with a rated supply voltage. Beyond the base speed, the flux speed product is held constant at the base speed ( $\omega_b$ ) value.

In this case, the machine is ramped up to speed using the speed reference after which it is subjected to a sequence of step changes in load torque. The following values are used:

tstop: The study time to two seconds.

time\_wref: The time array of the speed reference repeating sequence signal source to [0 0.5 tstop].

speed\_wref: The value array of the speed reference repeating sequence signal source to [0 wbm wbm].

time\_tmec: The time array of the  $T_{mech}$  repeating sequence source to [0 0.75 1.25 1.25 1.5 1.5 2].

tmec\_tmec: The value array of the  $T_{mech}$  repeating sequence source to [0 0-Trate -Trated/2-Trated/2 Trated -Trated 0 0]. Sampling Time: 2e-6 sec. One can see from Fig.(7) the monotonic response of the flux before it reaches its steady-state value (122.44 volt) compared to that oscillatory one in Fig.(6). Also, it is easy to see in Fig.(7) how well the flux amplitude remains constant when the motor is loaded, as compared to a large change in the flux response with open loop situation.

Another comparison is clear between the electromechanical torque responses of Fig.(7) and (6). The torque shows a smooth response in case of IFOC, while it is oscillatory in open loop case. The validity of IFOC technique is verified via two tests. In the first test, a change in stator quadrature current is generated by a repeating sequence source with the time and output values scheduled as follows:

$$\text{time\_change\_iqse} = [0 \ 0.6 \ 0.8 \ 0.9 \ 2]$$

$$\text{output\_change\_iqse} = [0 \ 0 \ 10 \ 10 \ 0]$$

and added to the commanded quadrature stator current in synchronous frame  $i_{qs}^{*e}$ . The same change values are fed to the direct stator current in synchronous frame  $i_{ds}^{*e}$  in the other test. The reflection of these changes on the output

synchronous qd components of the stator currents,  $i_{ds}^e$  and  $i_{qs}^e$ , and then to what extent the IFOC technique performs the decoupling action is investigated in Fig. (8).

In both tests, the machine is ramped up to mechanical base frequency  $\omega_{bm}$  in 0.5 second and started up at no load condition.

In Fig.(8), the change in  $i_{qs}^{*e}$  immediately appears at its corresponding output,  $i_{qs}^e$ , while no change is detected in  $i_{ds}^e$  and rotor flux magnitude  $|\psi_r|$ . Also, the figure shows the change in the response of developed torque and rotor speed due to this current change thus, the observations seen in Fig. (8) give a strong indication that the decoupling action is well performed by IFOC technique and the machine is, by now, a dc like machine. However, the conclusion that induction machine model has been converted to dc like machine is not yet decisive. There is still a problem behind the calculation of slip frequency, where the changes in rotor resistance could cause degradation in IFOC technique performance and the coupling effect might again be arisen (detuning effect).

### 3.Simulation of IFOC IM with Detuning Effect

The examination of detuning effect in the rotor resistance is performed by introducing an estimation factor,  $k_r$ , to all the  $r_r'$  terms of machine model. As set up, perfect tuning is when  $k_r=1$ . The previous run of perfect tuning, Fig.(7), is repeated at fixed reference speed (ramped up to speed  $\omega_{bm}$  in 0.5 sec) for a  $k_r=1.5$  and 0.5, with no-load, rated load and with cyclic change of load.

In the next study, the machine is subjected to the same sequence of step changes in load torque as previously applied in perfect tuning, Fig.(7). As compared to the perfect tuning case, the increased value of rotor resistance ( $1.5r_r'$ ) could cause the responses of flux linkages, torque and current to be distorted, especially, at time of load exertion,. Also, at this time the speed deviation from its steady state value is larger than the case with  $kr=1$ .

## CONCLUSIONS

The implementation of IFOC technique has been performed and the following observations could be concluded:

1. The technique can keep the rotor flux constant even during changes in load torque.
2. It has been shown that decoupling is conditioned by the accuracy of slip calculation. The slip calculation depends on the rotor time constant,  $T_r$ , which varies continuously according to the operational conditions.
3. On the other hand, the conventional PI controller can not compensate such parameter variations in the plant. That is, the PI controller is not an intelligent controller nor is the slip calculation accurate. Therefore, changes in  $T_r$  degrade the speed performance and other controllers can be suggested.

**REFERENCES**

1. Bimal K. Bose, "Modern Power Electronics and AC Drive," University of Tennessee, Knoxville, Prentice Hall, 2002.
2. Chee-Mun Ong, "Dynamic Simulation of Electric Machinery Using Matlab/Simulink", Purdue University, Prentice Hall PTR, 1998.
3. Dal Y. Ohm, "Dynamic Model of Induction Motors for Vector Control", Drivetech, Inc., Blacksburg, Virginia, 2001.
4. W. Leonhard, "Control of Electrical Drives," Springer Press, Berlin, 1998.
5. A. Ouhrouche and C. Volat, "Simulation of a Direct Field-Oriented Controller for an Induction Motor Using MATLAB/SIMULINK Software Package", Proceeding of the IASTED International Conference Modeling and Simulation, Pennsylvania, USA, May 15-17, 2000.
6. J.M.D. Murphy, F.G. Turnbull, "Power Electronic Control of AC Motors," Pergamon Press, 1988
7. G. Esmaily, A. khodabakhshian, K. Jamshidi, "Vector Control of Induction Motors Using UPWM Voltage Source Inverter", Faculty of Engineering, Isfahan, university, Isfahan, Iran, 2003.
8. Bimal K. Bose, "High Performance Control of Induction Motor Drives", Department of Electrical Engineering, The University of Tennessee, Knoxville USA, 1998.
9. Robert D. Lorenz, Thomas A. Lipo, and Donald W. Novotny, "Motion Control with Induction Motors", Proceedings of the IEEE, Vol. 82, No. 8, August 1994.

10. P. Vas, "Electrical Machines and Drives, A Space-Vector Theory Approach," Clarendon Press, Oxford, 1992.
11. M. A. Ouhrouche "EKF-Based On-Line Tuning of Rotor Time-Constant in an Induction Machine Motor Vector Control," International Journal of Power and Energy Systems, Vol.20, No.2, 2000.
12. Pui Yan Chung, Melik D. Ien, Robert D. Lorenz, "Parameter Identification for Induction Machines by Continuous Genetic Algorithms", University of Wisconsin ANNIE 200 Conference, November 5 – 8, 2000.
13. Amjad J. H., "Fuzzy learning enhanced speed control of indirect field orientation controlled induction machine with adaptive hysteresis band current controller", PHD thesis, University of Technology, Al-Rashid college of Engineering and Science, June, 2005.
14. Math Works, Inc., "SIMULINK user's Guide," Version 2, Jan 1997.
15. "Short Tutorial on Matlab," Tomas Co., 2004.

**Table 1: Induction Motor Parameter**

Rated Power	20 hp
Rated Line-Line Voltage	200 V
Rate Torque	81.5 Nm
Number of Poles (P)	4
Stator Resistance (rs)	0.106 Ω
Stator Inductance (L <sub>s</sub> )	9.15 mH
Magnetizing Inductance(L <sub>m</sub> )	8.67 mH
Rotor Resistance(r <sub>s</sub> )	0.076 Ω
Rotor Inductance (L <sub>s</sub> )	9.15 mH

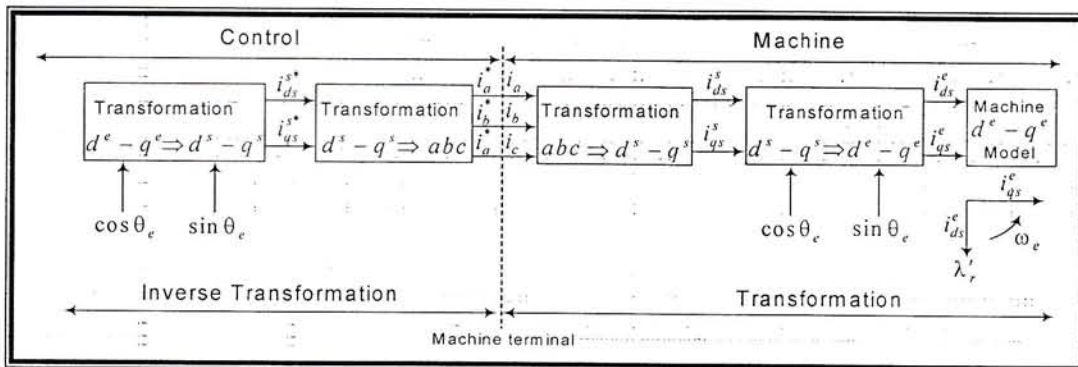


**Figure (1) Vector control implementation principle with machine**

*d<sup>e</sup> - q<sup>e</sup> model*

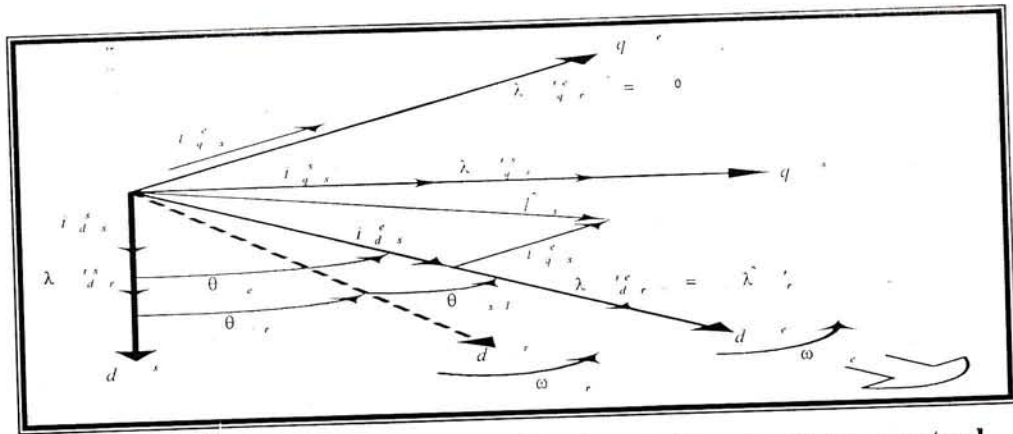


Figure (2) Phasor diagram explaining indirect vector control

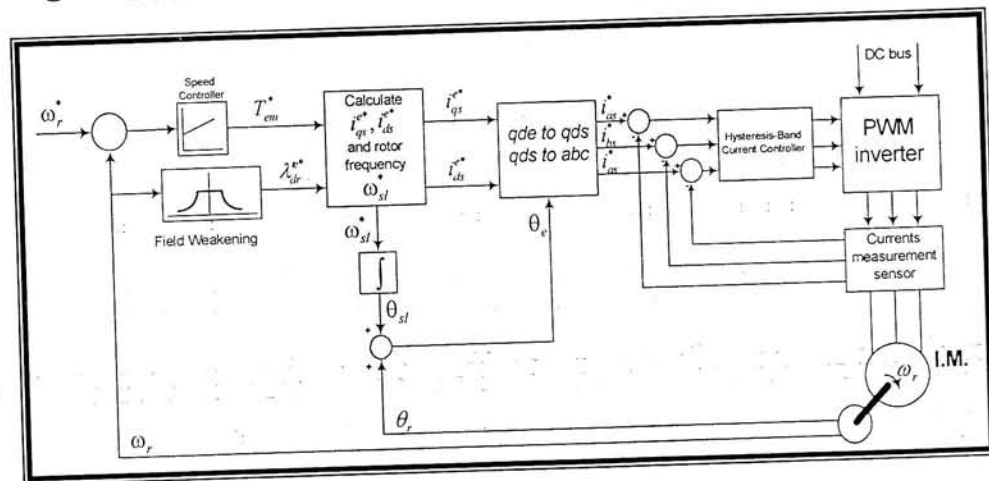


Figure (3) Indirect field-oriented control of a current regulated pwm

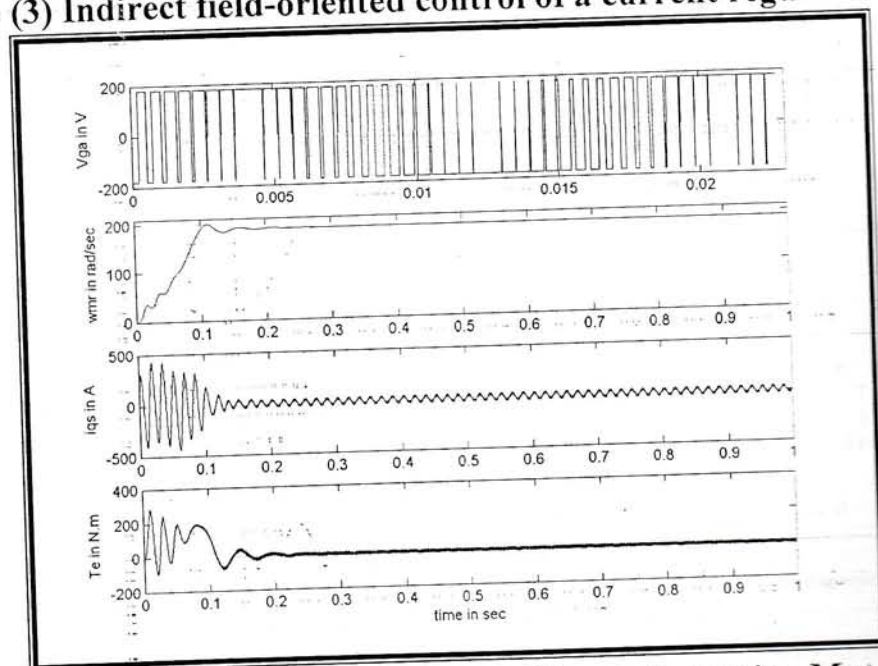


Figure (4) No-Load Response of Stationary Frame Induction Motor Model



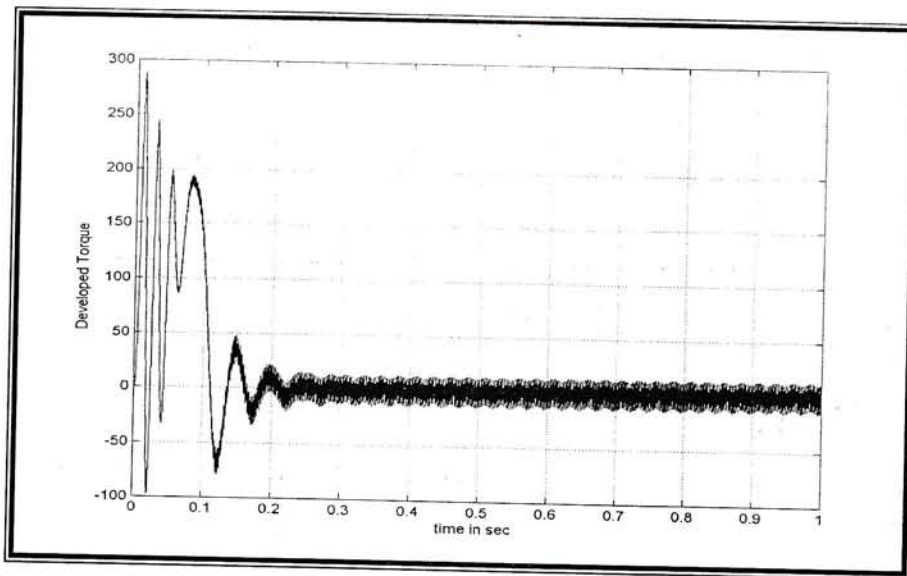
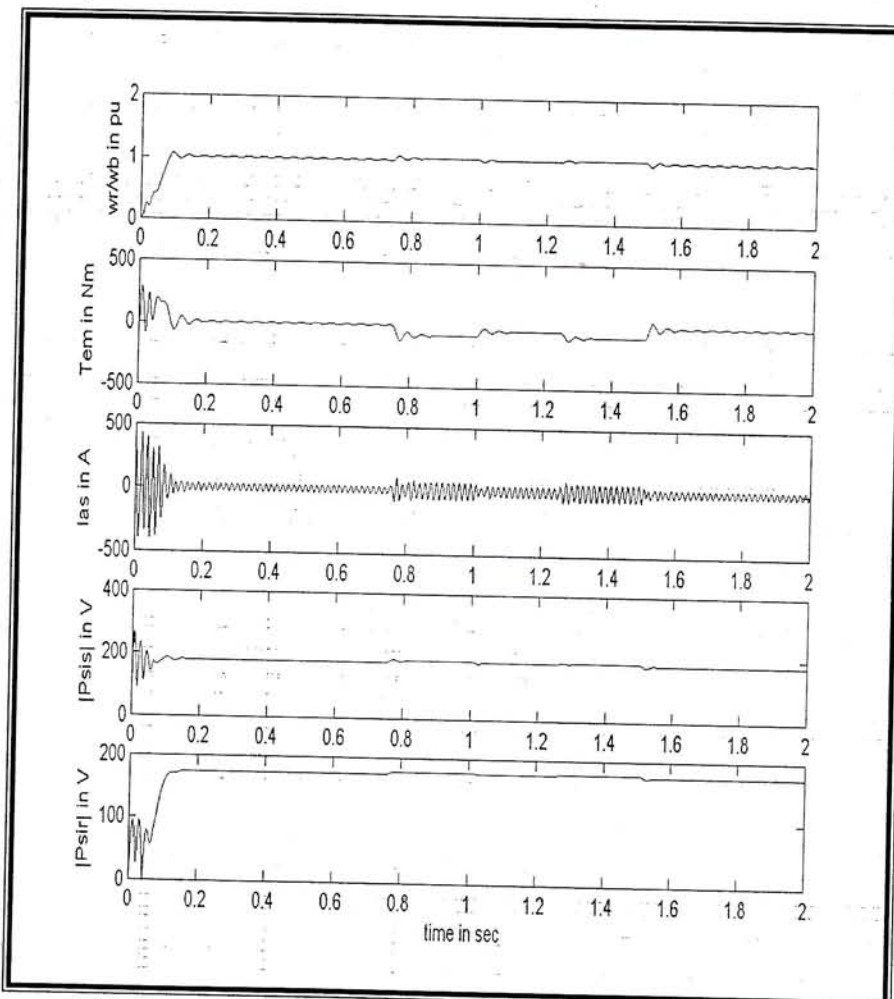


Figure (5) open loop torque-speed curve



Figure(6) Startup and cyclic loading of the IM model at no-load..

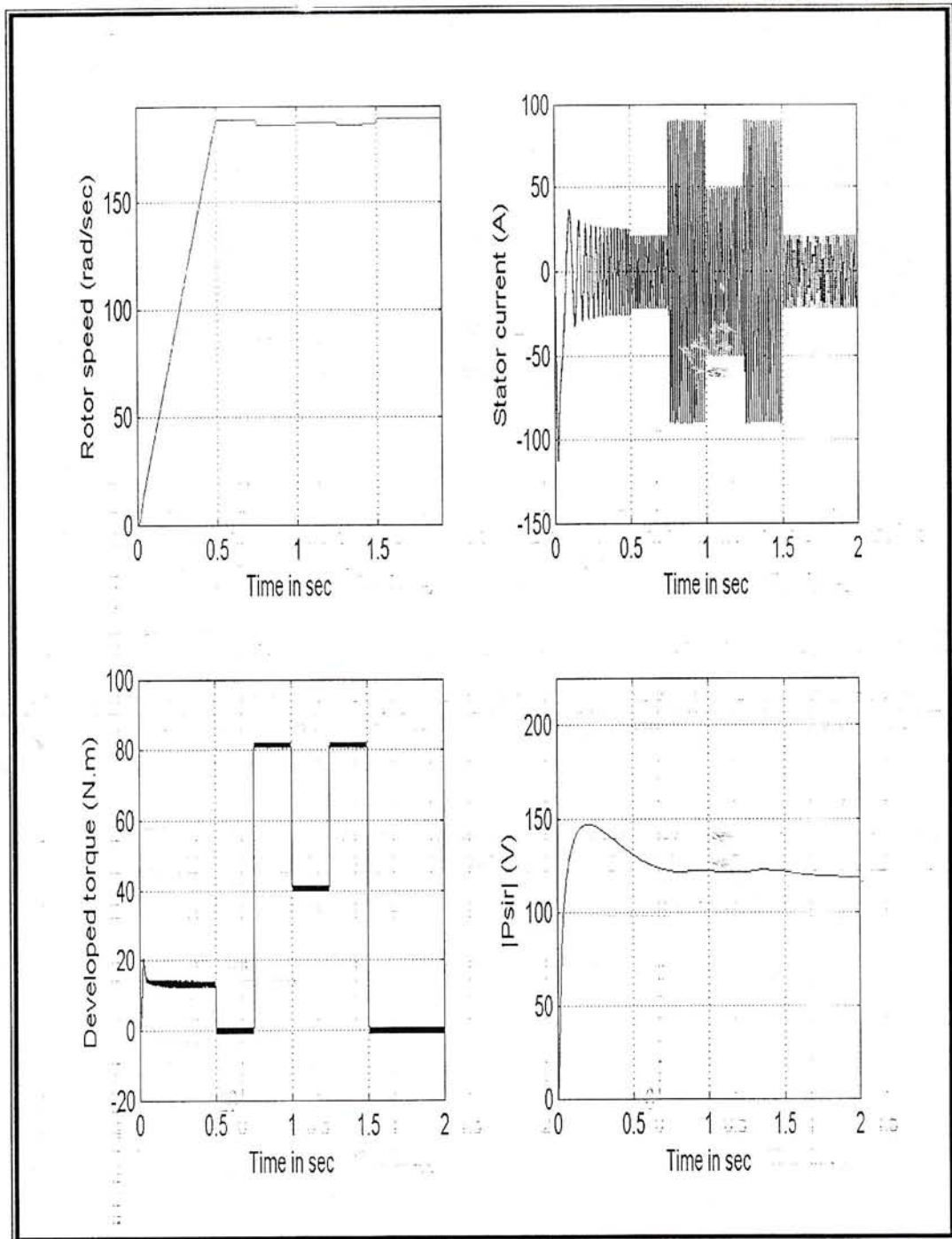


Figure (7) Startup and load transients with field-oriented control

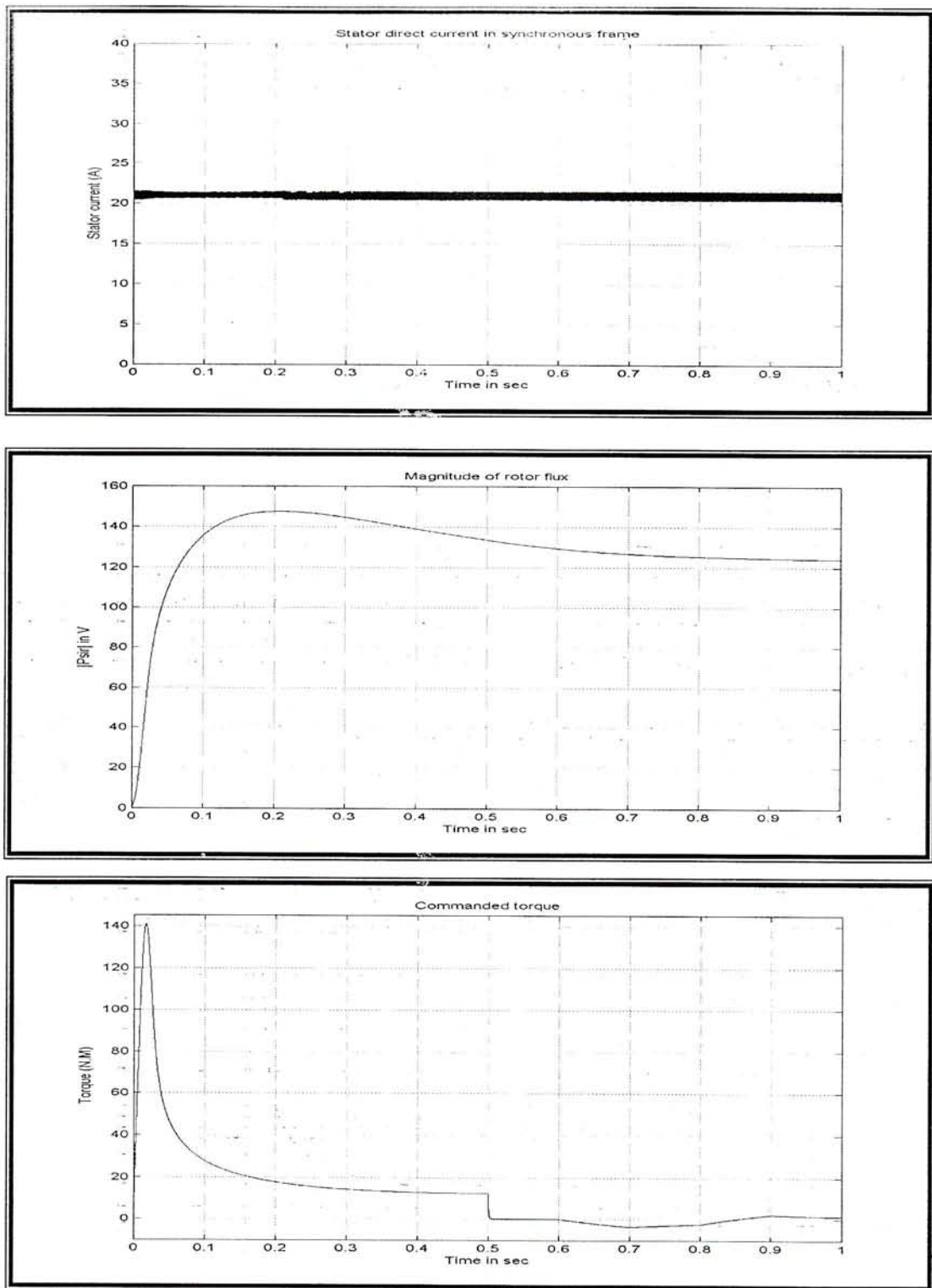


Figure (8) Changes in Responses due to a change in  $i_{qs}^*$

## السيطرة بتوجيه المجال الغير مباشر لماكنة الحث بتأثير تعيير دارة التنغيم

خلف سلوم كعيد الشمري

مدرس مساعد

قسم الهندسة الكهربائية-جامعة تكريت

### الخلاصة

المحركات الحثية توصف بالتعقيد، بانها غير خطيه ،وبان حركتها متغير مع الزمن صعوبة وصول بعض الحالات والنواتج للمقاييس التي قد تعتبر من حالات التحدي للمحركات الحثية. طرق السيطرة بتوجيه المجال للمحركات الحثية تحقق الفصل بين العزم وميكانيكية الفيض مما يؤدي الى استقلالية السيطرة للعزم وكذلك الفيض في حالة كون محرك التيار المستمر يعمل بفيض مفصول لكنها حساسة لتغيرات عناصر المحرك. هذا العمل هو طريقة السيطرة بتوجيه المجال الغير مباشرة لماكنة الحث بتأثير اعادة التنغيم هي طريقة فعالة لفصل هذا الترابط الحاصل. النتائج المعروضة تبين بوضوح مدى نجاح هذه الطريقة ومدى تحسن الاداء باستخدام هذه الطريقة في السيطرة

### الكلمات الدالة

المكائن الحثية، السيطرة بتوجيه المجال، السيطرة بتوجيه المجال الغير مباشر، طرق السيطرة على المتجه، توجيه الفيض الدوار، التخطيط الطوري، تأثير فصل التناغم، المسيطر الاعتيادي، السيطرة باعادة الفصل.